

# Tribological Conditions in Hot Bending of 22MnB5 Tubes



Enrico Simonetto, Andrea Ghiotti, and Stefania Bruschi

**Abstract** Thanks to the high stiffness-to-weight ratio given by the closed-section geometry, tubular components are particularly suitable for automotive applications that require extreme lightness to reduce energy consumption and increase crash-worthiness. Tube bending processes are traditionally performed in cold conditions, but to overcome the dramatic problems of accuracy and formability that the new high-strength steels present, a novel draw bending set at high temperature has been proposed. This paper presents the results of the investigations carried out on the tribological conditions of the hot draw bending of 22MnB5 tubes to obtain tubular parts with tailored mechanical properties. Investigation about the process thermal cycle has been performed with focus on the influence of the contact pressure on the heat transfer. The results show the practicability of the new process chain to obtain hot stamped tubular parts.

**Keywords** Tube draw bending · High-strength steels · Heat transfer

## 1 Introduction

The most recent trends of sustainable mobility require the reduction of the hazardous pollutants related to engine emissions. To this aim, the reduction of vehicle weight to decrease the fuel consumption and to increase their autonomy still represents a challenge due to strong requirements in terms of frame stiffness and passenger safety [1]. The last decade saw the development of several manufacturing technologies to further fulfil these needs. The hot stamping of High-Strength Steel (HSS) sheets was one of the most successful ones as it allowed increasing the geometrical complexity

---

E. Simonetto · A. Ghiotti (✉) · S. Bruschi

Department of Industrial Engineering, University of Padua, via Venezia 1, 35131 Padua, Italy

e-mail: [andrea.ghiotti@unipd.it](mailto:andrea.ghiotti@unipd.it)

E. Simonetto

e-mail: [enrico.simonetto.1@unipd.it](mailto:enrico.simonetto.1@unipd.it)

S. Bruschi

e-mail: [stefania.bruschi@unipd.it](mailto:stefania.bruschi@unipd.it)

© The Minerals, Metals & Materials Society 2021

G. Daehn et al. (eds.), *Forming the Future*, The Minerals, Metals & Materials Series, [https://doi.org/10.1007/978-3-030-75381-8\\_6](https://doi.org/10.1007/978-3-030-75381-8_6)

of the components and, at the same time, tailoring their final microstructure [2]. In this way, it made it possible to significantly reduce the thickness of body-in-white sheet components and therefore their weight [3]. A further improvement may be achieved by changing the design of many vehicle parts by substituting sheet-based components with tubular profiles. This could increase the component strength-to-weight ratio, thanks to the better mass distributions allowed by closed hollow cross-sections [4]. Tube bending processes are traditionally carried out at room temperature showing strong limits when applied to HSS such as (i) high forming loads, (ii) low formability, and (iii) high springback. While the former point can be solved by increasing the power of the bending machine actuators, the others limit both the complexity of the obtainable shapes and the accuracy of the processes and their repeatability. As of now, there are not any industrially available technologies to produce bent HSS tubes hardened during the process [5, 6] and with tailored microstructure and mechanical properties [7]. This paper presents experimental investigations carried out to assess the feasibility of new Direct Hot Bending (DHTB) processes of 22MnB5 tubes with focus on the thermal cycle and on the thermal boundary conditions that affect the final workpiece mechanical properties. Experimental measurements of the cooling rates that can be achieved in typical DHTB processes are carried out to evaluate the Heat Transfer Coefficients (HTC) with the tools. The results of the bends performed in hot conditions show that the proposed apparatus allows bending the HSS workpiece exploiting the increased formability of the austenite microstructure. Furthermore, the bent tubes show that different microstructures were obtained on different points according to the applied thermal boundary conditions.

## 2 Materials

The material used in the investigation is the 22 MnB5 steel grade, provided a sheet with 2 mm thickness and straight tubes having an outer diameter of 40 ( $\pm 0.1$ ) mm and a thickness of 2 ( $\pm 0.05$ ). The chemical properties are reported in Table 1.

The tool steel grade is the EN X38CrMoV5-1 alloyed steel, commercially available with the name Böhler W300 (nominal chemical composition in Table 2). To

**Table 1** Nominal chemical composition of a 22MnB5 tube (mass content in %)

Material	C	Mn	Si	Cr	Ti	B
22MnB5	0.21–0.25	1.1–1.4	0.15–0.35	0.15–0.30	0.02–0.05	0.003–0.005

**Table 2** Nominal chemical composition of the tool grade (mass content in %)

C	Si	Mn	P	S	Cr	Mo	Ni	V
0.39	0.97	0.43	0.015	0.006	5.01	1.14	0.21	0.35

improve its wear resistance at the hot stamping temperatures, the tool steel is heat-treated to the hardening temperature of 1040 °C and then oil-quenched to obtain a surface hardness of 51 ( $\pm 1$ ) HRC.

### 3 Direct Hot Tube Bending (DHTB)

A novel apparatus specifically developed for the rotary draw bending at high temperature of 22MnB5 tubes is hereafter presented. The apparatus is based on a traditional cold tube Rotary Draw Bending (RDB) machine, see Fig. 1, to assess the feasibility of the tube Direct Hot Tube Bending (DHTB) process. Figure 1 shows the main tools and kinematics of RDB.

#### 3.1 DHTB Equipment

A resistance heating system is embedded within the bending machine, in order to limit the thermal loss during the handling stage, and to have the maximum flexibility in the application of thermal cycles to different zones of the tube. A DC generator with a maximum power of 60 kW (6000 A at 10 V) is used as a heating device as shown by Fig. 2a. Two couples of copper electrodes connect the tube with the DC generator; these can be opened or closed to grip the tube, by means of two pneumatic actuators with a maximum force of 950 N each. A couple of electrodes is mounted on a fixed frame (see Fig. 2b), positioned near the pressure die to limit the distance between the heating zone and the dies, to decrease both the handling time and the

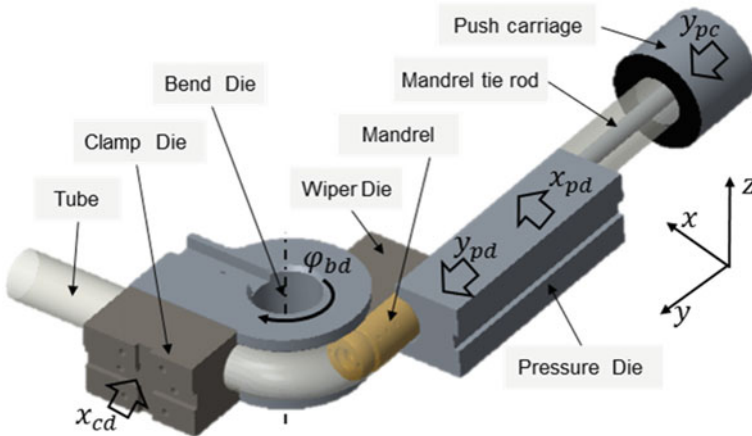


**Fig. 1** Kinematics and tools in rotary draw bending process. (Color figure online)

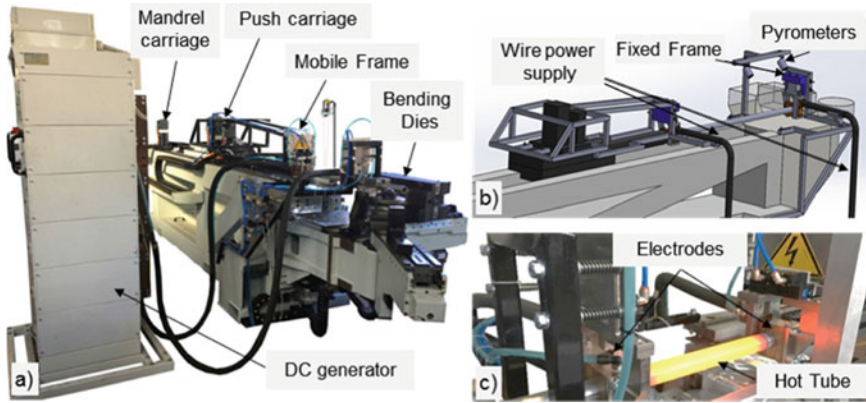


**Fig. 2** **a** Overall view of the bending machine equipped with the heating apparatus for DHTB process, **b** model of the heating electrodes, and **c** hot tube heated by resistance heating. (Color figure online)

minimum distance between two subsequent bends. The other couple of electrodes is mounted on a mobile frame linked to the push carriage. This design allows moving the electrodes along the tube axis to change the heated length and adjust the length of the heat-treated zone to the bend angle. The tube temperature is monitored in-line by means of a pyrometer during the heating and holding stages allowing to control the applied electrical power in a closed-loop configuration. Figure 2c shows the copper electrodes and the tube heated at 950 °C during the austenitization stage. This solution has been preferred to others, such as induction heating, since it allows greater flexibility in terms of heating length without hindering the handling stages. The equipment has been tested, by heating the 22MnB5 tubes up to 950 °C, with a heating rate of 5.25 °C/s and a holding time of 60 s with different heated length, namely 200, 300, 400, and 500 mm, to assess the temperature gradient along the treated zone.

### 3.2 Thermal Cycle

By applying a thermal field to the workpiece, it is possible to (i) increase the material formability to obtain more complex shapes, (ii) to reduce the springback angles, and (iii) modify the steel microstructure and so the mechanical properties. To achieve these results, the thermal cycle applied to the tube must be controlled. Figure 3 shows the proposed thermal cycle for the DHTB process, which includes the following steps:

- i. Austenitization stage: the tube is heated up until ( $T_{Aust}$ ) over the Austenitization temperature ( $A_{c1}$ ) to obtain an austenitic structure. The heating rate can be increased and so the heating time reduced according to the capabilities of the power supply, in order to reduce the overall process time, while the holding

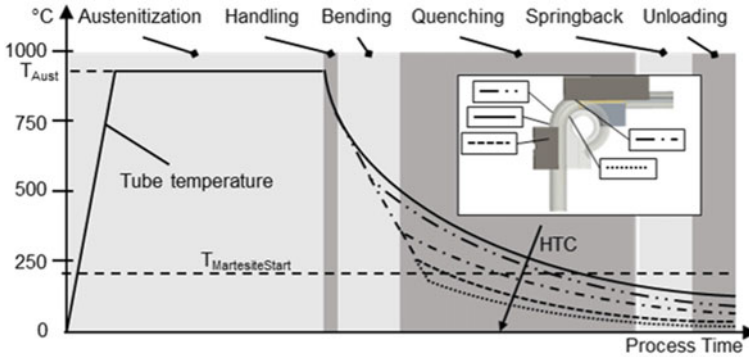


**Fig. 3** Thermal cycle applied during the subsequent DHTB process stages. (Color figure online)

time at  $T_{Aust}$  is a function of the material properties in order to obtain a partially or fully austenitic structure according to the desired final mechanical properties of the component.

- ii. Handling stage: the heated zone is moved from the heating system to the dies group in order to bend the tube. This stage is particularly critical as it is necessary to limit heat loss.
- iii. Bending stage: the tube is bent while its temperature is still inside the process temperature window. In fact, all the forming stage should be completed while the tube microstructure is still austenite in order to allow an increased formability. At the end of the process, the mandrel is withdrawn from the bending zone.
- iv. Quenching stage: after the bending stage is over, the tube is not unloaded as the tools are kept closed in order to maintain higher cooling rates.
- v. Springback: when the tube cools down under the lower martensite transformation temperature, in order to reach the highest mechanical strength, the forming loads are released and the tube undergoes the springback phenomenon. However, the springback effect is greatly reduced by the thermal effects.
- vi. Unloading: the bent zone is unloaded from the bending machine.

### 3.3 Boundary Conditions

As shown from the process model in Fig. 1, the thermal boundary conditions during the bending and quenching stages are not constant along the bent zone as the tools move during the process. Consequently, the thermal boundary conditions are not constant during the process forming stage. The chart in Fig. 3 shows different cooling paths that different points along the bending zone undergo during the process according to the evolution of the thermal boundary conditions. Figure 4 shows the contact conditions along several sections of the bending zone, in different moments of the bending stage. At the beginning of the bending stage, as shown by Section

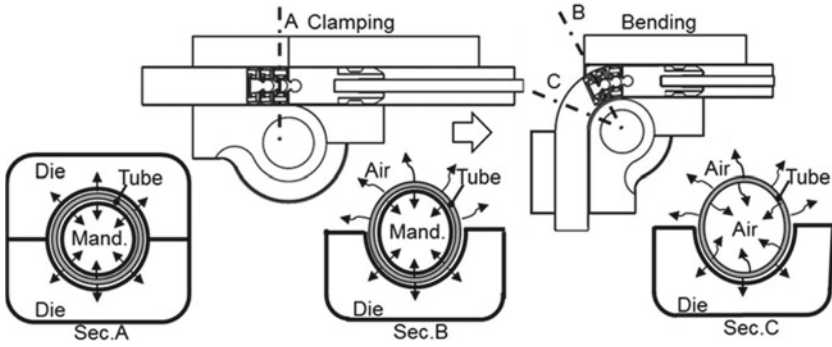


Fig. 4 Main boundary conditions during the quenching stage

A, the thermal exchange is mainly due to conduction since both the inner and outer tube surfaces are in contact with the dies or with the mandrel. Sections B and C are considered after the bending: in the former, the tube inner surface is still in contact with the mandrel and the tube intrados is in contact with the bend die but it is exposed to the air at the extrados. In the latter, the tube is in contact only with the bend die at the intrados, while there is air at the extrados and inside the tube. Therefore, the thermal conditions change during the bending stage and are different point by point, making the process difficult to control.

### 3.4 HTC Equipment

Figure 5a shows the developed experimental setup to test the different heat transfer conditions between the boron steel specimens and the dies, and between the boron

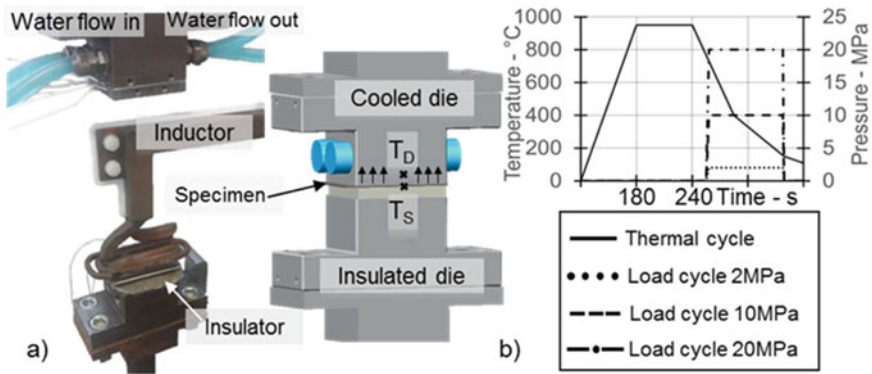


Fig. 5 a) Experimental setup and the 3D model of the apparatus, b) load and thermal cycles of the cooling tests. (Color figure online)

**Table 3** Experimental plan

Case	1	2	3	4	5	6	7
Normal pressure (MPa)	0	2	10	20	2	10	20
Cooling condition	Calm air	Metal die	Metal die	Metal die	Cooled die	Cooled die	Cooled die
Fluid temperature (°C)	20	–	–	–	10	10	10
Flow per channel (l/s)	–	–	–	–	0.3	0.3	0.3

steel specimen and the air. A 22MnB5 flat sample (size equal to  $45 \times 50 \times 2$  mm) is heated by a frontal inductor head, according to the thermal cycle shown in Fig. 5b. The volume and the thickness of these flat samples are consistent with the dimension of the tube bent zone, to replicate a sample with similar thermal inertia and thermal boundary conditions.

Both the die temperature ( $T_D$ ) and the specimen temperatures ( $T_S$ ) are measured during the entire test by K-type thermocouples. To replicate the air cooling on the inner surface and with the bending tool on the outer surface, an insulating layer of trathermic® Silcem 1300 is interposed between the specimen and the lower die. Both dies are manufactured with the Böhler W300 steel as indicated in Sect. 2, with embedded cooling channels. The dies are mounted on a hydraulic press MTS322®, capable of a maximum load of 50 kN. The equipment was used to perform different cooling tests, according to Table 3, applying different levels of normal pressure consistent with the values undergone by the tube during the process. The tests were carried out with and without water flow on the upper die channels.

## 4 Numerical Model

To determine the heat transfer coefficients between the 22MnB5 sheet and the dies, a numerical inverse analysis was performed [8]. Figure 6a shows the 3D numerical model, developed with the commercial software Forge Nxt™, while Fig. 6b shows the temperature profile of the 22MnB5 sheet when the measured temperature  $T_S$  reaches the  $T_M$  value for a pressure of 2 MPa without water cooling. The thermal exchange between the sheet and the cooled die has been determined in order to fit the simulated temperature with the cooling paths measured during the real tests.

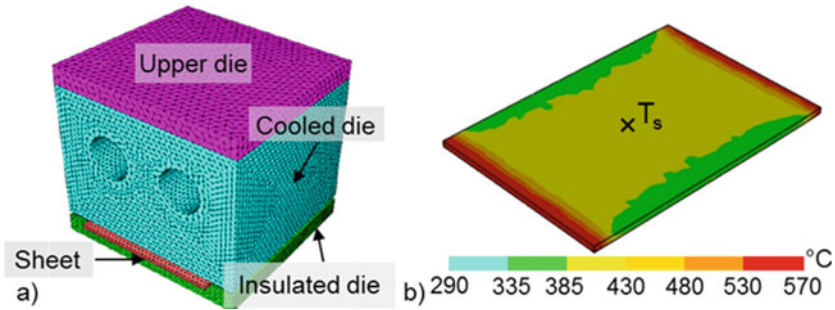


**Fig. 6** a) 3D numerical model of the test system, b) sample temperature profile when reaching the phase changing temperature  $T_M$  on the measuring point  $T_S$  (Case 2). (Color figure online)

## 5 Results

### 5.1 Thermal Profile

The typical austenitization process for the 22MnB5 requires a temperature of 950 °C, and so the electrodes are water-cooled below 100 °C to avoid excessive oxidation. As the cooled electrodes are in contact with the tube, also the tube is cooled down leading to a certain thermal gradient along the heated length as shown in Fig. 4c. A FLIR™ A40 infrared thermal-camera (measurement range 20–1200 °C) was used to assess the temperature distribution along the tube axis for different heating lengths. Figure 7 shows its distribution for different lengths: 200, 300, 400, and 500 mm. It is possible to notice that the central part of the heated zones has a constant and uniform temperature, with a maximum deviation of  $\pm 5$  °C, while the end zones of the tubes are at lower temperature due to the presence of the cooled electrodes. The length of these transient zones near the electrodes has a constant value of 50 ( $\pm 10$ ) mm.

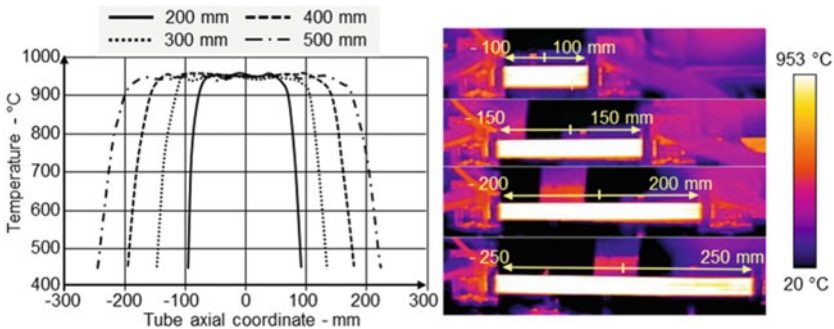


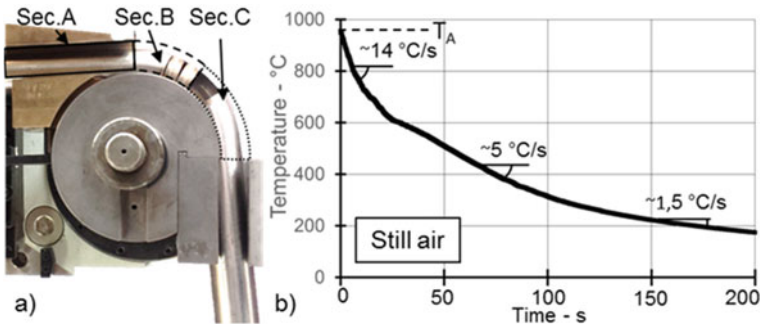
**Fig. 7** Temperature profile along the tube axis at the end of the austenitization stage for different heated length. (Color figure online)



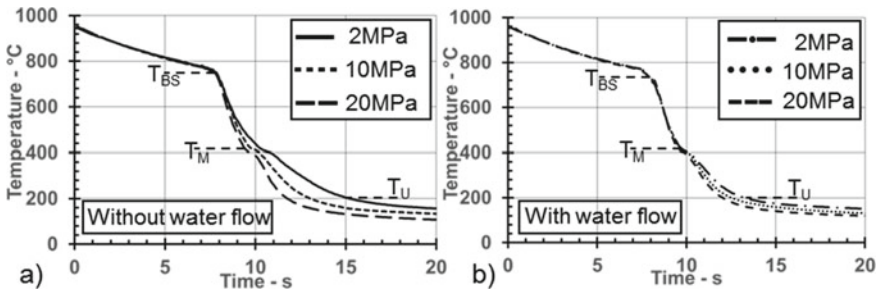
### 5.2 HTC Determination

Figure 8 shows the cooling rate obtained in still air. Figure 8a shows the bent tube at the end of the forming process, where the outer tube surface in the extrados cools down in still air, as shown by Sections B and C in Fig. 3. The cooling path in still air starts from  $T_A$ , see Fig. 8b, which is the temperature after the heating. It is worth noticing that the slope change around 600 °C is due to the latent heat release during the bainitic transformation.

The cooling paths measured during the die cooling tests are shown in Fig. 9. The first part of the cooling corresponds to the transfer time from the heating zone to the bend dies, starting from  $T_A$  down to the bending starting temperature  $T_{BS}$ . Then the dies are closed, with different pressures, leading to a faster temperature drop until  $T_M$ . The dies are then kept closed until the unloading temperature  $T_U$  is reached. In the case of water-cooled dies, the contact pressure between the dies and the specimen is less influential as shown in Fig. 9b.



**Fig. 8** a Tube and tool position at the end of the bending step, b specimen cooling path in still air from austenitization temperature. (Color figure online)



**Fig. 9** a Specimen cooling path in die cooling without water flow, b specimen cooling path in die cooling with a water flow of 0.3 l/s per channel

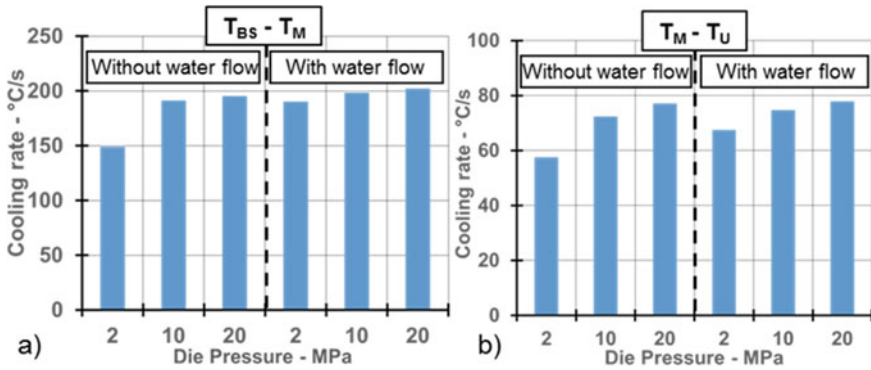
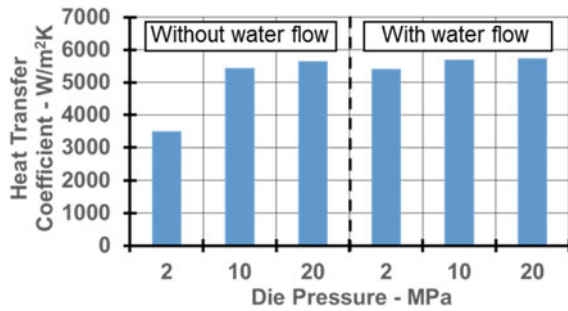


**Fig. 10** a Cooling rates measured in die cooling tests, from TBS to TM, b cooling rates measured in die cooling tests, from TM to TU. (Color figure online)

**Fig. 11** Heat transfer coefficient obtained from the inverse analysis from  $T_{BS}$  to  $T_U$  for the die cooling conditions. (Color figure online)



The measured cooling paths were used to calculate the cooling rate varying both the contact pressure and the cooling conditions of the dies. Figure 10a shows the different cooling rates measured before the martensitic transformation while Fig. 10b shows the cooling rate down to  $T_U$ .

The experimental data were used to calculate the HTC's, see Fig. 11, between the die and the specimen by the numerical reverse analysis as discussed in Sect. 4. It was seen that HTC is almost stable for contact pressure values over 10 MPa without water flow, while it appears almost negligible with proper water flow.

### 5.3 Process Time

The duration of each process stages affects the thermal cycle and leads to changes in the workpiece final properties. As discussed in Sect. 3, the tube must be bent before any changes in the microstructure occur in order to avoid any loss of formability or increase in forming loads due to the presence of Martensite or Bainite. Figure 12 shows the position of the bending machine main axes during the process, starting

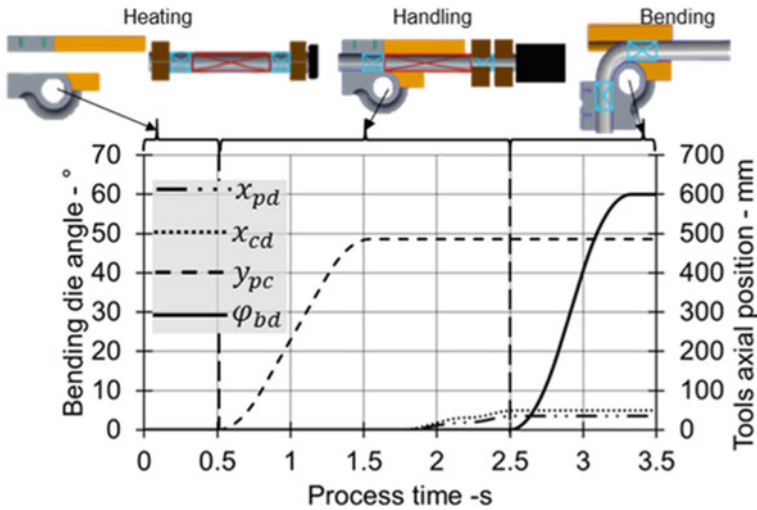


**Fig. 12** Position of the bending machine main axes during the DHTB process. (Color figure online)

from the end of the Austenitization stage when the workpiece reaches the thermal profile shown in Fig. 7. During the handling stage, the pneumatic actuators open the copper electrodes and the tube gripped by the push carriage is moved along the axial direction to take the heated zone in the bending position; this operation requires 1.25 s. As shown in Fig. 4, the tube is gripped by the bend and clamp dies in the transient zones as this part is not deformed during the process, while the zone of the tube uniformly heated at 950 °C is positioned between the pressure and the wiper die to be bent. When the tube is in the right axial position, the dies are brought into contact with it, in 0.75 s as shown in Fig. 12. Then the tube is bent with an angular rate of 80°/s, taking 0.75 s to perform a 60° bend as reported in the chart. The cooling rate in still air for a 2 mm thickness tube can be estimated around 15 °C/s while in the case of cooling rate due to conductivity with a die, the cooling rate reaches maximum values of 200 °C/s for a pressure of 20 MPa. Therefore, as the tube is cooled in still air for 0.75 s and then it is in contact with the dies for 1.5 s until the end of the bending state, it is possible to say that the bending operation can be safely carried out before any microstructural changes occur within the tube.

#### 5.4 Mechanical Properties

After the bending stage the tube is cooled inside the dies, but during the quenching stage different zones of the bent tube undergo different cooling rates. The differences between the thermal boundary conditions on the tube intrados and extrados lead to non-uniform cooling rates and so different final microstructures are obtained. Figure 13a shows a bent tube by means of the DHTB process and highlights two

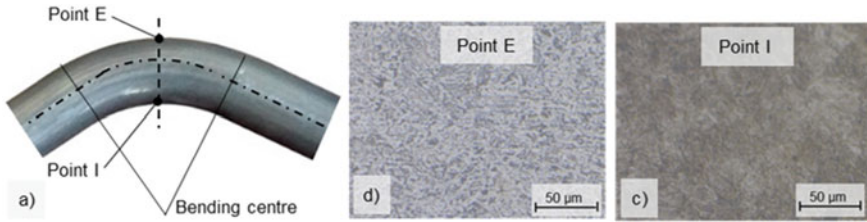


**Fig. 13** a Tube bent with DHTB process, b microstructure at the extrados side, and c microstructure at the intrados side. (Color figure online)

different points on the extrados (Point E) and intrados (Point I). The microstructures of these two points were analysed showing that on the extrados side (Point E) a ferrite-perlite-based structure is still present due to the low cooling rate (Fig. 13b). On the other hand, Fig. 13c shows the martensitic microstructure obtained in point I, thanks to the highest cooling rate, greater than the  $27\text{ }^{\circ}\text{C/s}$  required to obtain the martensitic transformation.

## 6 Conclusions

This paper presents an investigation about the Tribological conditions in Direct Hot Bending of a hollow profile. In particular, it focuses on the thermal cycle and on the influence of the thermal boundary conditions between the workpiece and the machine tools. A DHTB prototype was developed to bend 22MnB5 after heating them up to the austenitization temperature, and a simplified experimental equipment was developed to determine the cooling rates and the HTC as a function of different process parameters. The developed prototype uses a DC generator linked to the workpiece by means of two couple of cooled copper electrodes to apply the thermal field using the Joule effect. The thermal profiles measured at the end of the heating stage, using an infrared thermal-camera, show how the developed system allows to heat up different workpiece lengths in a homogeneous way, with a transition zone of  $50 (\pm 10)$  mm near the electrodes. Furthermore, the cooling rate and HTCs between the workpiece, the environment, and the dies were determined using the experimental equipment presented in Sect. 5.2 as a function of the contact pressure and of the die cooling channel water flow. These data, together with the process time measured in the DHTB operation allowed to estimate the process temperature windows. The process time was minimized to perform the forming operation at high temperature avoiding any phase transformation and any related formability decrease due to microstructural changes. Then the final microstructures of two different reference points were analysed to evaluate the influence of the different thermal boundary conditions, along the bent tube. The results show that two different microstructures are obtained, as a consequence of the different thermal boundary conditions, in particular a martensitic

structure was obtained on the intrados side, while a ferrite-perlite-based structure was obtained on the bend outer side. The technology proved to be promising to manufacture bent tube with tailored microstructure and mechanical behaviour.

## References

1. Tekkaya AE, Khalifa NB, Grzanic G, Holker R (2014) Forming of lightweight metal components: need for new technologies. *Procedia Eng* 81:28–37
2. Bariani PF, Bruschi S, Ghiotti A, Turetta A (2008) Testing formability in the hot stamping of HSS. *CIRP Ann* 57:265–268
3. Merklein M, Wieland M, Lechner M, Bruschi S, Ghiotti A (2016) Hot stamping of boron steel sheets with tailored properties: A review. *J Mater Process Technol* 228:11–24
4. Hea Y, Heng L, Zhiyong Z, Mei Z, Jing L, Guangjun L (2012) Advances and trends on tube bending forming technologies. *Chinese J Aeronaut* 1–12
5. Hu Z, Li JQ (1999) Computer simulation of pipe-bending processes with small bending radius using local induction heating. *J Mater Process Technol* 91:75–79
6. Zhang XL, Yang H, Li H, Zhang ZY, Li L (2014) Warm bending mechanism of extrados and intrados of large diameter thin-walled CP-Ti tubes. *Trans Nonferrous Met Soc China* 24:3257–3264
7. Simonetto E, Venturato G, Ghiotti A, Bruschi S (2018) Modelling of hot rotary draw bending for thin-walled titanium alloy tubes. *Int J Mech Sci* 148:698–706
8. Simonetto E, Bruschi S, Ghiotti A, Savio E (2015) Prediction of distortions in hot forged martensitic stainless steel turbine blades by numerical simulation. *Procedia Manuf* 1:804–813